Tomáš Gotthans

NONLINEAR DYNAMICAL SYSTEMS

BRNO UNIVERSITY OF TECHNOLOGY

Faculty of Electrical Engineering and Communication

Department of Radio Electronics

Field of Research

ELECTRONICS AND COMMUNICATION

Ing. Tomáš Gotthans, Ph.D.

NONLINEAR DYNAMICAL SYSTEMS

NELINEÁRNÍ DYNAMICKÉ SYSTÉMY

SHORT VERSION OF HABILITATION THESIS

KEYWORDS

Nonlinear system, power amplifier, Volterra series, power series, polynomial series, error vector magnitude, adjacent channel power ratio, normalized mean square error.

KLÍČOVÁ SLOVA

Nelineární systém, výkonový zesilovač, Volterrovy řady, mocninné řady, polynomiální řady, velikost vektoru chyby, poměr výkonu sousedního kanálu, normalizovaná střední kvadratická odchylka.

MÍSTO ULOŽENÍ HABILITAČNÍ PRÁCE:

Contents

1. About the Author

Ing. Tomáš Gotthans, Ph.D.

born	January 26, 1985
e-mail	gotthans@feec.vutbr.cz

Current position

since 2014   *Researcher*
at FEEC BUT with specialization in nonlinear modeling, signal processing, power amplifier design and physical layer of mobile communication

Qualification

2014   Docteur, Université Paris-Est Marne la Vallée,
L'École Doctorale Mathématiques et Sciences et Technologies de l'Information et de la Communication
2010   Ing., Electronics and Communication,
Brno University of Technology

Research

Nonlinear dynamical systems, linearization and modeling of power amplifiers, physical layer of mobile communication
Web of Science h-index: 6
Scopus h-index: 7 (ID: 41761598800)
Papers indexed by Google Scholar:
 https://scholar.google.cz/citations?user=GKCJZWoAAAAJ&hl=cs
ORCID:
 https://orcid.org/0000-0002-0386-1813

Internships

2016	Instituto de Telecomunicações (Portugal) – 2 months
2015	ESYCOM laboratory, Paris (France) – 1 month
2011-2014	ESIEE Engineering Paris (France) – 3 years

Personal skills

Languages   Czech – mother tongue
English – fluent
French and German – basic knowledge

2. Introduction

Research described in this thesis has been carried out at Department of Radio Electronics, Brno University of Technology. It has been done in cooperation mainly with several other colleagues - prof. Geneviève Baudoin, prof. Roman Maršálek, prof. Markus Rupp, doc. Jiří Petržela, dr. Jiří Blumenstein and doctoral students Ing. Jan Král, Ing. Martin Pospíšil and Michal Harvánek.

It is common situation that nonlinear devices are simulated using computers. There can be complex models modelling physical phenomenas of each electronic part. Models on physical level are usually very complex and difficult to handle even with modern computers. Another approach can be modeling systems in fact as a black-box device.

Another aspect of non-linear systems is the reduction and modeling of inconvenient effects connected with a real characteristic of many real-world parts [18], especially the modeling aspects connected with non-linear power amplifiers (PA) used in wireless communications and broadcasting.

Power amplifiers are critical elements of mobile communication and broadcasting systems because their efficiency conditions the autonomy and the weight of mobile handset batteries and their linearity influences on performance of the communication. In practice, PAs are not perfectly linear and present memory effects, i.e. the output signal is a function of the current and of previous input signal values. And a compromise must be achieved between the efficiency and the linearity of the PA [11].

The aim of this work is to bring new innovative solutions to improve the performance of RF power transmitters. The work conducted in this thesis is a part of work for the project AMBRUN (FUI project with partners: Thales, TeamCast, Supélec and ESIEE Paris). The project aimed to improve the radio performance of the amplification of multiplexed signals using adaptive algorithms for dual applications: tactical communication and broadcasting VHF band. The originality and ambition of the project lie in the bandwidths of processed signals (above 40 MHz) the involved powers (up to 100W) and the non-stationarity of tactical multiplex signals.

An increasing demands on communications system with every generation of devices. One may observe, that in 1985 for AMPS systems the required bandwidth of signal was 30kHz. Comparing for example with the latest LTE Advanced, that can require 100MHz of bandwidth. The LTE Advanced requires approximatively 3400 times larger bandwidth than AMPS systems. And for future 5G systems (high speed, low latency), the bandwidth expectations are in range of 1 GHz. That is also challenging in terms of signal processing.

3. Techniques For Analyzing And Modeling Non-linear Systems

This chapter presents the principals models that can be used for modelling PA or for digital predistortion (DPD). It is composed of two main parts: first the description of the models, then the methods for identification of the models. It focuses on models that can be used in the case of PA linearization.

There are several models used in modeling the PA (or used for DPD) from the simplest models modelling just the amplitude distortions to the most general form known as Volterra series and its derivatives.

We may distinguish the models to three basic categories: memoryless or static, quasi-static and dynamic (or memory) models. For memoryless models, the output at time t only depends on input at time t and it can be shown that the system introduces only amplitude distortions. These amplitude distortions only depends on the magnitude of the input signal. Quasi-static models can also model phase distortions depending on the signal magnitude.

The third category is called dynamic, because these models are able to model memory effects.

3.1 Static and Quasi-static models

3.1.1 Memoryless RF Polynomial Series

One of the most straightforward models are the polynomial series. We can define the RF model for power amplifier as:

$$y_{RF}(t) = \sum_{n=1}^{N} a_n x_{RF}^n(t). \tag{3.1}$$

The coefficients of models can be obtained from simple measurements such as P_{L1dB}, IP3; etc. Let us establish the baseband equivalent model of the RF polynomial series.

Let us investigate the behavior in the presence of n-th order nonlinearity [5]:

$$x_{RF}^n(t) \quad = \quad \frac{1}{2^n} \left[x(t)e^{j\omega_0 t} + x^*(t)e^{-j\omega_0 t} \right]^n \tag{3.2}$$

$$= \quad \frac{1}{2^n} \sum_{k=0}^{n} \binom{n}{k} x(t)^k x^*(t)^{(n-k)} e^{j\omega_0(2k-n)t}.$$

We are interested by $y_{RF1}(t)$ that is the component at frequency $\pm f_0$. So we look for component for which:

$$(2k - n) = \pm 1. \tag{3.3}$$

For n even, $(2k - n)$ never equals 1, therefore $\omega_0(2k - n)$ is always out of band. For n odd the frequencies can be in-band. Hence (for $-\omega_0$) we may write:

$$k \quad = \quad \frac{n-1}{2}, \tag{3.4}$$

$$(n - k) \quad = \quad \frac{n-1}{2} + 1.$$

Then using (3.5) we may define:

$$x(t)^k x^*(t)^{n-k} \quad = \quad x(t)^{\frac{n-1}{2}} x^*(t)^{\frac{n-1}{2}+1} \tag{3.5}$$

$$= \quad |x(t)|^{n-1} x(t)^*.$$

Similarly for frequency $+f_0$ for $(2k - n) = 1$ we obtain:

$$x(t)^k x^*(t)^{n-k} \quad = \quad |x(t)|^{n-1} x(t). \tag{3.6}$$

Using these results the baseband output is defined as:

$$y(t) = \sum_{\substack{n=1 \\ n \text{ odd}}}^{N} \frac{a_n}{2^{n-1}} \binom{n}{(n-1)/2} |x(t)|^{n-1} x(t), \tag{3.7}$$

setting

$$b_n = \frac{a_n}{2^{n-1}} \binom{n}{(n-1)/2}. \tag{3.8}$$

This explains why the baseband models are often defined with odd coefficients only. They can be defined as:

$$y(t) = \sum_{\substack{n=1 \\ n \text{ odd}}}^{N} b_n x(t) |x(t)|^{n-1} = \sum_{k=0}^{\frac{N-1}{2}} b_{2k+1} x(t) |x(t)|^{2k}, \tag{3.9}$$

where x is the input baseband signal of the power amplifier, y is the output baseband signal of PA and b_n are the polynomial coefficients.

Another explanation why equivalent baseband models contain only odd terms can be done using Shimbo formula [20, 19]. For the rest of the thesis we will refer only to baseband models of PA (the PA is followed by bandpass filter).

In practice including even order terms in baseband models can improve performance.

Several models corresponding to modeling the AM/AM and AM/PM characteristic have been given, for example: Saleh, Rapp, quasi-static models. Their general expression is given by:

$$y(t) = A(|x(t)|)e^{j\phi(|x(t)|)}x(t). \tag{3.10}$$

We precise some of them in the following sections.

3.2 Dynamical Models Derived From Volterra Series

3.2.1 Polynomial series with memory

Polynomial memory series (PMS) were first presented in [12] and are widely used for modeling the non-linearities [6, 5, 16]. They can be interpreted as a special case of a generalized Hammerstein model. The presented series can model the memory effects. In this model, all off-diagonal terms of the Volterra series are set to zero. The series is defined as:

$$
\begin{aligned}
y(t) &= \sum_{k=1}^{K}\sum_{q=0}^{Q} b_{kq}\, x(t-q)|x(t-q)|^{k-1} \\
&= \sum_{k=1}^{K}\sum_{q=0}^{Q} b_{k,q}\Phi_{k,q}(x(t)) = \mathbf{\Phi}(t)\mathbf{b},
\end{aligned}
\tag{3.11}
$$

where

$$
\begin{aligned}
\Phi_{k,q}(x(t)) &= |x(t-q)|^{k-1}x(t-q), & (3.12) \\
\mathbf{b} &= [b_{1,0}, b_{2,0}, ..., b_{1,1}, ..., b_{1,Q}, ..., b_{K,Q}]^{T} & (3.13) \\
\mathbf{\Phi}(t) &= [\Phi_{1,0}(x(t)), ..., \Phi_{K,Q}(x(t))]. & (3.14)
\end{aligned}
$$

Their structure is determined by 2 parameters: K the non-linearity order and Q the memory length. The number of coefficients is $K(Q+1)$.

These models have good performance for applications with narrow or medium bandwidths. But they are often insufficient when large bandwidth applications are needed because of their limitation in modeling memory effects. For large bandwidth applications more complicated models are necessary.

3.2.2 Dynamic Deviation Reduction Models

To overcome the complexity of the general Volterra series, an effective model pruning method, called dynamic deviation reduction (DDR) [2, 13, 1] was proposed. It is based on the fact that the effects of dynamics tend to fade with increasing nonlinearity order in many real PAs, so that the high-order dynamics can be removed in the model, leading to a significant simplification in model complexity.

Note that this dynamic-order truncation does not affect the nonlinearity or memory truncation in the same way as in the classical series. In other words, it only removes higher order dynamics, preserving the static nonlinearities and low-order dynamics[2].

The 2st-order dynamic truncation of the DDR-based baseband Volterra model in the discrete time can be written as:

$$
\begin{aligned}
y(t) = {} & \sum_{k=0}^{\frac{K-1}{2}} \sum_{i=1}^{Q} g_{2k+1,1}(i)\, |x(t)|^{2k} x(t-i) \\
& + \sum_{k=1}^{\frac{K-1}{2}} \sum_{i=1}^{Q} g_{2k+1,2}(i)\, |x(t)|^{2(k-1)} x^2(t) x^*(t-i) \\
& + \sum_{k=1}^{\frac{K-1}{2}} \sum_{i_1=1}^{Q} \sum_{i_2=1}^{Q} g_{2k+1,3}(i_1,i_2)|x(t)|^{2(k-1)}\, x^*(t)x(t-i_1)x(t-i_2) \\
& + \sum_{k=1}^{\frac{K-1}{2}} \sum_{i_1=1}^{Q} \sum_{i_2=1}^{Q} g_{2k+1,4}(i_1,i_2)|x(t)|^{2(k-1)}\, x(t)x^*(t-i_1)x(t-i_2) \\
& + \sum_{k=1}^{\frac{K-1}{2}} \sum_{i_1=1}^{Q} \sum_{i_2=1}^{Q} g_{2k+1,5}(i_1,i_2)|x(t)|^{2(k-2)}\, x^3(t)x^*(t-i_1)x^*(t-i_2).
\end{aligned} \tag{3.15}
$$

where $x(n)$ and $y(n)$ are the complex envelopes of the input and output of the PA, respectively, and $g_{2k+1,j}$ is the complex Volterra kernel of the system.

A simplified version of the model is defined by:

$$
\begin{aligned}
y(t) = {} & \sum_{k=0}^{\frac{K-1}{2}} \sum_{i=0}^{Q} g_{2k+1,1}(i)\, |x(t)|^{2k} x(t-i) \\
& + \sum_{k=1}^{\frac{K-1}{2}} \sum_{i=1}^{Q} g_{2k+1,2}(i)\, |x(t)|^{2(k-1)} x^2(t) x^*(t-i) \\
& + \sum_{k=1}^{\frac{K-1}{2}} \sum_{i=1}^{Q} g_{2k+1,3}(i)|x(t)|^{2(k-1)}\, x(t)|x(t-i)|^2 \\
& + \sum_{k=1}^{\frac{K-1}{2}} \sum_{i=1}^{Q} g_{2k+1,4}(i)|x(t)|^{2(k-1)}\, x^*(t)x^2(t-i).
\end{aligned} \tag{3.16}
$$

3.2.3   Generalized Memory Polynomials

Another model including cross terms is the generalized memory polynomials (GMP)[17]. Inserting a delay of samples between the signal and its exponentiated envelope using positive and negative cross-term time shifts we get:

$$
\begin{aligned}
y(n) \;=\;& \sum_{k=0}^{K_a-1} \sum_{l=0}^{L_a-1} a_{k,l} x(n-l)|x(n-l)|^k \\
&+ \sum_{k=1}^{K_b} \sum_{l=0}^{L_b-1} \sum_{m=1}^{M_b} b_{k,l,m} x(n-l)|x(n-l-m)|^k \\
&+ \sum_{k=1}^{K_c} \sum_{l=0}^{L_c-1} \sum_{m=1}^{M_c} c_{k,l,m} x(n-l)|x(n-l+m)|^k,
\end{aligned}
\tag{3.17}
$$

where the structure of GMP models is determined by 8 parameters: K_a, K_b, K_c non-linearity orders, L_a, L_b, L_c memory lengths and M_b, M_c distances from the diagonal of Volterra series, and $a_{k,l}$, $b_{k,l,m}$ and $c_{k,l,m}$ are the linear coefficients of the equation.

In order to reduce the complexity, it is not necessary in many cases to use all of the co-efficients. For example, odd-order nonlinearities usually dominate so that we may only want to consider odd-order terms. Also additionally, depending on the signal bandwidth and sampling rate, it may not be necessary to implement all cross-term time shifts.

3.3   Identification of Models

In this section we will focus on models with linear dependency with respect to their coefficients. The interest of these models is that we will obtain a convex minimization problem for the least-squares (LS) criteria for PA modeling and DPD with indirect learning architecture.

In order to identify the coefficients of PA model or DPD coefficients, we use LS optimization criterion:

$$
\mathbf{e} = \min_b ||\mathbf{y} - \mathbf{z}||^2.
\tag{3.18}
$$

We apply notations defined in Fig.3.1, where for PA modeling $y(t)$ is measured signal (for DPD $x(t)$ is measured signal) and $z(t)$ is the output of the model. We consider here only indirect learning approach for the DPD.

The $||.||^2$ represent the quadratic norm of vector and $\mathbf{z}$ is expressed as:

$$
\mathbf{z} = \mathbf{U}\mathbf{b},
\tag{3.19}
$$

and where a $\mathbf{z}$ is a in vector with dimensions $N \times 1$:

$$
\mathbf{z} = [z(0), ..., z(N-1)]^T.
\tag{3.20}
$$
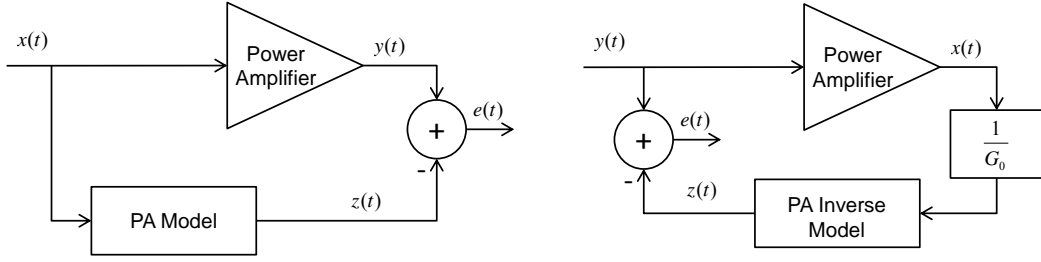
Figure 3.1: Schematic of minimizing problem between measured and modeled signals. The left schematic represents calculation of PA model. The right schematic represents calculation of PA inverse model (note that the input $x(t)$ and output $y(t)$ notation is swapped in order to meet error defined in (3.18).

$$\mathbf{y} = [y(0), ..., y(N-1)]^T. \tag{3.21}$$

$$\mathbf{e} = [e(0), ..., e(N-1)]^T. \tag{3.22}$$

As seen in equation (3.19) $\mathbf{U}$ is a matrix of size $N \times N_c$ (where N_c represents number of coefficients and for example for PMS $N_c = K(Q+1)$):

$$\mathbf{U} = \begin{pmatrix} \mathbf{\Phi}(0) \\ \mathbf{\Phi}(t) \\ \vdots \\ \mathbf{\Phi}(N-1) \end{pmatrix}. \tag{3.23}$$

$\mathbf{b}$ a vector of size $N_c \times 1$

$$\mathbf{b} = [b_0, ..., b_{N_c-1}]^T. \tag{3.24}$$

The optimization problem can be written:

$$\min_{\mathbf{b}}(\mathbf{e}^H\mathbf{e}). \tag{3.25}$$

3.3.1 Least Squares one-shot solution

The LS solution minimizing distance between each data point and the space of best fit passing through the data points for (3.19). The criteria $\mathbf{J}$ can be expressed as:

$$\mathbf{J(b)} = ||\mathbf{z} - \mathbf{y}||^2 = \mathbf{e}^H\mathbf{e} = (\mathbf{y} - \mathbf{Ub})^H(\mathbf{y} - \mathbf{Ub}) \tag{3.26}$$

$$= \mathbf{b}^H\mathbf{U}^H\mathbf{Ub} - \mathbf{y}^H\mathbf{Ub} - \mathbf{b}^H\mathbf{U}^H\mathbf{y} + \mathbf{y}^H\mathbf{y}$$

The solution of (3.27) can be obtained by calculating the gradient and setting it to 0. The gradient is equal to:

$$\frac{\partial \mathbf{J((b))}}{\partial \mathbf{b}} = 2\,\mathbf{U}^H\mathbf{Ub} - 2\,\mathbf{U}^H\mathbf{y}, \tag{3.27}$$

The least square solution yields to:

$$\mathbf{U}^{H}\mathbf{U}\mathbf{b} - \mathbf{U}^{H}\mathbf{y} = 0. \tag{3.28}$$

$$\mathbf{b} = (\mathbf{U}^{H}\mathbf{U})^{-1}\mathbf{U}^{H}\mathbf{y} = \mathbf{U}^{+}\mathbf{y}, \tag{3.29}$$

where $\mathbf{U}^{+}$ denotes Moore - Penrose pseudo-inverse. The LS algorithm is in fact one-shot solution for block of data.

LS one-shot solution is quite good in terms of performance. Nevertheless an interest in adaptive algorithms grows (adaptive filtering, adaptive equalization, etc.). The problem with LS one-shot solution is, that it is not able to track PA variations. Therefore adaptive algorithms have been proposed for the case of DPD identification either.

3.3.2 Damped Newton Algorithm

In many applications, adaptive estimation is performed on a block by block basis. There exists method called Damped Newton Algorithm (DNA) that upgrades the LS solution by adding possibility to control the speed of convergence depending on the preceding error. The DNA works block by block and it adapts preceding vector of coefficients to take into account the new block of data with a damping factor. In this section we will
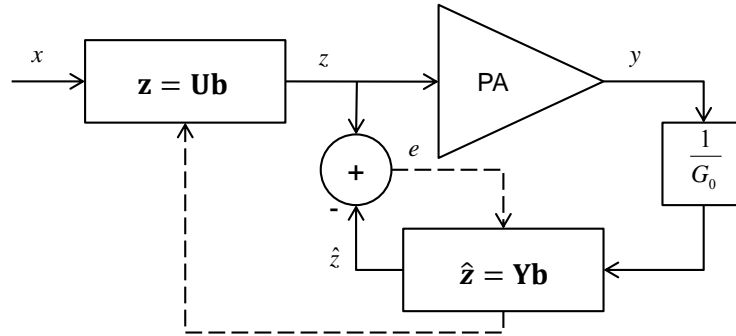
Figure 3.2: Schematic of DNA system.

The initialization vector $\mathbf{b}_0$ is usually chosen to use predistorter as a transparent block as:

$$\mathbf{b}_0 = [1, 0, \cdots, 0]^{T}. \tag{3.30}$$

According to notation in Fig.3.2 we can describe the algorithm for $n \in 1, 2, 3, ...$, where n represents the block number, with the following equation for block n (each block has N samples):

$$\mathbf{z} = \mathbf{U}\,\mathbf{b}_{n-1}. \tag{3.31}$$

Equivalently as in (3.20-3.23) we define the output matrix $\mathbf{Y}$ from the signal $\frac{y}{G_0}$ as:

$$\hat{\mathbf{z}} = \mathbf{Y}\,\mathbf{b}_{n-1}. \tag{3.32}$$

Then we define the error vector $\mathbf{e}$

$$\mathbf{e} = \mathbf{z} - \hat{\mathbf{z}}. \tag{3.33}$$

The coefficients $\mathbf{b}$ can be updated as:

$$\mathbf{b}_n = \mathbf{b}_{n-1} + \mu \left(\mathbf{Y}^H\mathbf{Y}\right)^{-1} \mathbf{Y}^H\,\mathbf{e}, \tag{3.34}$$

where μ is a relaxation variable. When setting the relaxation variable $\mu = 1$ the damping is removed and the solution becomes the standard LS solution.

3.3.3 LMS algorithm

The Least Mean Square (LMS) algorithm is often used in adaptive systems due its simplicity and relative precision. The algorithm works sample by sample. The algorithm computes instantaneous error and then corrects the actual value of coefficients.

Using any of models defined before with linear relation with respect to their coefficients (for example PMS, OMPS, DDR) we note:

$$\mathbf{\Phi}(n) = n^{th} \; row \; of \; matrix \; \mathbf{U}. \tag{3.35}$$

Then the criterion function can be defined as:

$$\begin{aligned} \min J(n) &= \; min\,|e(n)|^2 \\ &= \; min\,|y(n) - \mathbf{\Phi}(n)\mathbf{b}(n)|^2\,. \end{aligned} \tag{3.36}$$

The estimated gradient vector becomes:

$$\nabla J(n) = \frac{\partial|e(n)|^2}{\partial\mathbf{b}(n)} \tag{3.37}$$

Because

$$e(n) = z(n) - \mathbf{\Phi}(n)\mathbf{b}(n), \tag{3.38}$$

applying equation (3.38) to equation (3.37) we get:

$$\nabla J(n) = -e(n)\mathbf{\Phi}^H(n). \tag{3.39}$$

Then using the steepest descent weight update equation we obtain iterative solution:

$$\mathbf{b}(n+1) = \mathbf{b}(n) + \mu e(n)\mathbf{\Phi}^H, \tag{3.40}$$

where parameter μ adjusts the compromise between convergence speed and the error value after convergence.

Due to sensitivity to value μ that can lead to instability, the algorithm was modified by using a normalization that improves stability of the algorithm. This algorithm is so-called Normalized Least Mean Square (NLMS) defined as:

$$\mathbf{b}(n+1) = \mathbf{b}(n) + \mu\,e(n)\,\frac{\mathbf{\Phi}^H}{\mathbf{\Phi}\,\mathbf{\Phi}^H} \tag{3.41}$$

Both LMS and NLMS suffers from low convergence speed and limited precision.

3.3.4 RLS algorithm

For solving the LS criterion optimization problem recursive least squares (RLS) algorithm can also be used. In its adaptive form it converges faster than LMS. Theoretically where the forgetting factor is equal to 1, it achieves the optimal solution (Wiener solution) but it is more complex than LMS. Now defining the input of the system:

$$\mathbf{x}(n) = [x(n), x(n-1), \ldots, x(0)]^T, \tag{3.42}$$

and vector of desired output:

$$\mathbf{y}(n) = [y(n), y(n-1), \ldots, y(0)]^T. \tag{3.43}$$

Then we define line vector $\boldsymbol{\Phi}(n)$ as before of size $1 \times N_c$ and matrix $\boldsymbol{\Theta}$ of size $(n+1) \times N_c$ as:

$$\boldsymbol{\Theta}(n) = \begin{pmatrix} \boldsymbol{\Phi}(0) \\ \vdots \\ \boldsymbol{\Phi}(n) \end{pmatrix}. \tag{3.44}$$

Then the output of the system will be:

$$\mathbf{z}(n) = \boldsymbol{\Theta}(n)\mathbf{b}(n). \tag{3.45}$$

The instantaneous error at time n is:

$$e(n) = y(n) - \boldsymbol{\Phi}(n)\mathbf{b}(n). \tag{3.46}$$

Now defining the criterion function with a forgetting factor denoted as λ:

$$
\begin{aligned}
\min_{\mathbf{b}} J(n) &= \sum_{k=0}^{n} \lambda^{n-k} |e(k)|^2 \\
&= \sum_{k=0}^{n} \lambda^{n-k} |y(k) - \boldsymbol{\Phi}(k)\mathbf{b}(n)|^2 \\
&= \mathbf{e}^H \boldsymbol{\Lambda} \mathbf{e}(n)
\end{aligned}
\tag{3.47}
$$

where:

$$\boldsymbol{\Lambda} = \mathrm{diag}\left[1, \lambda, \lambda^2, \ldots, \lambda^n\right] \tag{3.48}$$

To use recursive implementation we need to define the correlation matrix $\mathbf{R}(n)$ by a recurrence equation:

$$
\begin{aligned}
\mathbf{R}(n) &= \boldsymbol{\Theta}^H(n)\boldsymbol{\Lambda}\boldsymbol{\Theta}(n) \\
&= \sum_{k=0}^{n} \lambda^{n-k} \boldsymbol{\Phi}^H(k)\boldsymbol{\Phi}(k) \\
&= \sum_{k=0}^{n-1} \lambda^{n-k} \boldsymbol{\Phi}^H(k)\boldsymbol{\Phi}(k) + \boldsymbol{\Phi}^H(n)\boldsymbol{\Phi}(n) \\
&= \lambda \mathbf{R}(n-1) + \boldsymbol{\Phi}^H(n)\boldsymbol{\Phi}(n).
\end{aligned}
\tag{3.49}
$$

We define the cross-correlation vector of size $N_c \times 1$:

$$
\begin{aligned}
\mathbf{p}(n) &= \mathbf{\Theta}^H(n)\mathbf{\Lambda}\mathbf{y}(n) \\
&= \sum_{k=0}^{n} \lambda^{n-k}\mathbf{\Phi}^H(k)y(k) \\
&= \sum_{k=0}^{n-1} \lambda^{n-k}\mathbf{\Phi}^H(k)y(k) + \mathbf{\Phi}^H(n)y(n) \\
&= \lambda\mathbf{p}(n-1) + \mathbf{\Phi}^H(n)y(n).
\end{aligned}
\tag{3.50}
$$

Defining the recursive solution:

$$
\mathbf{b}(n+1) = \mathbf{R}^{-1}(n)\mathbf{p}(n) = \mathbf{P}(n)\mathbf{p}(n),
\tag{3.51}
$$

where defining $\mathbf{P}(n) = \mathbf{R}^{-1}(n)$ and applying the inversion lemma to calculate $\mathbf{R}^{-1}(n)$ yields to:

$$
\mathbf{P}(n) = \lambda^{-1}\mathbf{P}(n-1) - \frac{\lambda^{-2}\mathbf{P}(n-1)\mathbf{\Phi}^H(n)\mathbf{\Phi}(n)\mathbf{P}(n-1)}{1 + \lambda^{-1}\mathbf{\Phi}(n)\mathbf{P}(n-1)\mathbf{\Phi}^H(n)}.
\tag{3.52}
$$

Now defining the gain $\mathbf{g}(n)$:

$$
\mathbf{g}(n) = \frac{\lambda^{-1}\mathbf{P}(n-1)\mathbf{\Phi}^H(n)}{1 + \lambda^{-1}\mathbf{\Phi}(n)\mathbf{P}(n-1)\mathbf{\Phi}^H(n)}
\tag{3.53}
$$

Then applying (3.53) to $\mathbf{P}(n)$ defined in (3.52) we get:

$$
\mathbf{P}(n) = \lambda^{-1}\mathbf{P}(n-1) - \lambda^{-1}\mathbf{g}(n)\mathbf{\Phi}(n)\mathbf{P}(n-1).
\tag{3.54}
$$

To rewrite the recursive weight update algorithm:

$$
\begin{aligned}
\mathbf{g}(n) &= \frac{\lambda^{-1}\mathbf{P}(n-1)\mathbf{\Phi}^H(n)}{1 + \lambda^{-1}\mathbf{\Phi}(n)\mathbf{P}(n-1)\mathbf{\Phi}^H(n)} \\
\mathbf{P}(n) &= \lambda^{-1}\mathbf{P}(n-1) - \lambda^{-1}\mathbf{g}(n)\mathbf{\Phi}(n)\mathbf{P}(n-1) \\
e(n) &= y(n) - \mathbf{\Phi}^T(n)\mathbf{b}(n) \\
\mathbf{b}(n+1) &= \mathbf{b}(n) + \mathbf{g}(n)e(n).
\end{aligned}
\tag{3.55}
$$

We define initial conditions as $\mathbf{p}(0) = 0$, $\mathbf{R}(0) = \delta\mathbf{I}$, where $\mathbf{I}$ is identity matrix. The typical value of δ is usually set as a small positive value equal to $\delta = 10^{-3}$. Then we can define:

$$
\mathbf{P}(0) = \mathbf{R}^{-1}(0) = \delta^{-1}\mathbf{I}.
\tag{3.56}
$$

To show the relationship between LS solution and RLS algorithm lets set $\lambda = 1$, we get:

$$
\mathbf{R}(n) = \mathbf{\Theta}^H(n)\mathbf{I}\mathbf{\Theta}(n).
\tag{3.57}
$$

$$
\mathbf{p}(n) = \mathbf{\Theta}^H(n)\mathbf{I}\mathbf{z}(n).
\tag{3.58}
$$

and using:

$$
\begin{aligned}
\mathbf{R}(n)\mathbf{b}(n) &= \mathbf{p}(n) \\
\mathbf{\Theta}^H(n)\mathbf{I}\mathbf{\Theta}(n)\mathbf{b}(n) &= \mathbf{\Theta}^H(n)\mathbf{I}\mathbf{z}(n).
\end{aligned}
\tag{3.59}
$$

we get:

$$
\mathbf{b}(n) = \left(\mathbf{\Theta}(n)\mathbf{\Theta}^H(n)\right)^{-1}\mathbf{\Theta}(n)\mathbf{z}(n).
\tag{3.60}
$$

We recognize (3.60) for $n = N$ the LS solution for the block of N samples.

Introducing a forgetting factor λ leads to an adaptive algorithm. RLS converges faster and is more precise than LMS. The RLS algorithm is more complex than LMS.

4. Analytical Method of Fractional Sample Period Synchronisation for Digital Predistortion Systems

Abstract

As the data throughput is still increased in the wireless communication systems, it is required to efficiently utilise the radio frequency spectrum which usually requires linear transmitters. Consequently methods as a digital predistortion (DPD) are developed to linearise nonlinear power amplifiers. To extract precise parameters for the DPD it is essential to finely synchronise measured feedback signal with the known transmitted signal. In this section we propose an analytical method for the fractional sample period time synchronisation suitable for DPD signals. Finally benefits of the proposed method are presented on results of its usage for the DPD linearisation using a measurement test-bed.

4.1 Introduction

As wireless communication systems develop higher demand is placed on data throughput and spectral and power efficiency. The higher data throughput and spectral efficiency is usually achieved using spectrally efficient modulations. The most of these modulations require usage of linear power amplifiers (PAs). These PAs are in principle low power efficient and in opposite high power efficient PAs are nonlinear. A technique solving this contradiction in modern communication systems is usage of a high power efficient nonlinear PA together with a digital predistorter (DPD). The DPD linearises characteristics of the nonlinear transmitter while preserving high power and spectral efficiency.

The typical implementation of the DPD is depicted by its baseband model in Fig. 4.1. The transmitter input and output signals are sampled, aligned, and processed to extract the DPD parameters that would be used to predistort the source signal before transmission to counteract the transmitter nonlinearities. However, the alignment accuracy in DPD is limited by nonideal electronic components and the associated circuitry which introduces unknown loop delay mismatch and thus degrades the overall linearisation performance as shown in Fig. 4.2 and in [8]. This section analyses the influence of the accuracy of the timing of these signals on the performance of the predistorter. It considers the case of an integer and a fractional delay (less than the sampling period). It is shown that for a predistorter without memory, even very small fractional offset degrades

performance significantly. The theoretical analysis by Liu [15] reveals that performance degradation caused by the loop delay mismatch increases as well with the bandwidth of the orthogonal frequency-division multiplexing (OFDM) signal.
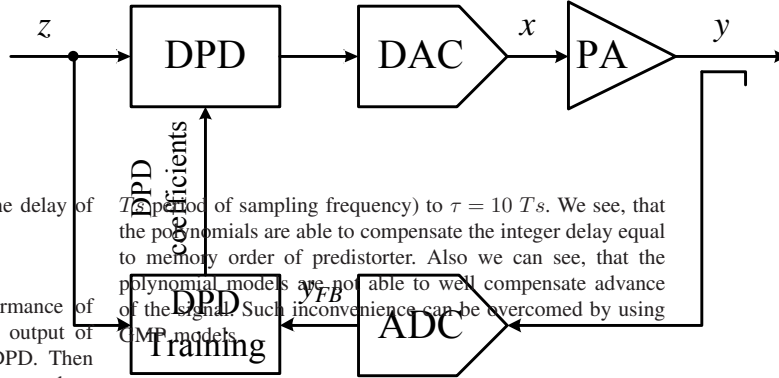
Figure 4.1: Baseband model of the digital predistorter

the bandwidth of the signal and τ is the delay of

IV. Used Method

...ate the influence of lag on the performance of ...rter we introduced fractional lags the output of ...ve used signals with misaligned for DPD. Then ...ed the performance of DPD and compared to ...ned without lag in the identification of DPD. For ...e evaluation we used normalized mean square error ...ween the output of the cascade DPD + PA and ... signal. For two signals **x** input and **y** output it is

$$NMSE(\mathbf{x}, \mathbf{y})[dB] = 10 \log \frac{\sum ||\mathbf{x} - \mathbf{y}||^2}{\sum ||\mathbf{x}||^2} \qquad (9)$$

...pect of our work is not only to correct the nonlin- ...oduced by power amplifier, but also simultaneously ...memory effects, integer and fractional lag.

V. Experimental Results

...nt results measured on Doherty amplifier UHF ...OS using BLF888A transistor (75W) used for ...lications(470 MHz to 860 MHz). As the useful ...ave used OFDM-like signal with the oversampling ...he amplifier has been modeled with orthogonal ... with nonlinearity order $K = 7$ and the memory ... We give here the results for a DPD with the same ...-linearity $K = 7$ and the memory M ranging from

T period of sampling frequency) to $\tau = 10\,Ts$. We see, that the polynomials are able to compensate the integer delay equal to memory order of predistorter. Also we can see, that the polynomial models are not able to well compensate advance of the signal. Such inconvenience can be overcomed by using GMP models.

B. Case of fractional delay

The fractional delay (in the meaning of non multiples of sampling periode Ts) can be introduced by mismatch of digital to analog and analog to digital converters and by the delay of power amplifier. Fig.4 shows the values NMSE with variable
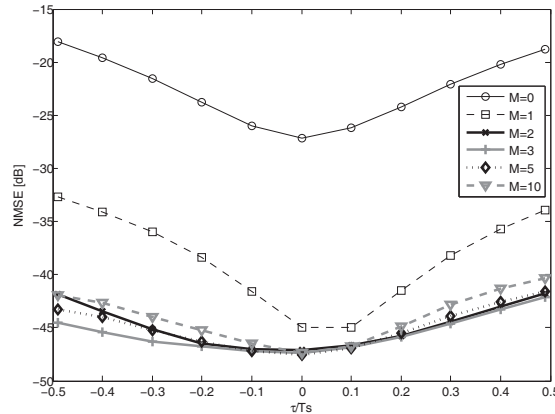
Figure 4.2: Effect of fractional delay for different memory length on normlised mean square error (NMSE) of the DPD with PA modelled by orthogonal polynomials with nonlinearity order $K = 7$ and the memory depth between 3 [8]

memory front 0 to 10 depending on the normalized fractional delay and $\tau = 0.5\,Ts$. We can see that the DPD is able to compensate for the fractional offset and nonlinearities. The usage of DPD with memory is very important and can increase the performance of coefficients. In the case of delay, the DPD with PA modelled by orthogonal polynomials with nonlinearity order $K = 7$ and the memory depth between 3 and $\tau = 0.5\,Ts$ delay, the memory is able to compensate fractional delay and also fractional advance.

As a consequence of the delay mismatch degradation, a precise time synchronisation method is required for the DPD implementation. Time synchronisation and recovery have been already widely explored in the communication theory. An algorithm for symbol timing recovery using baud-rate sampling is described in [3]. Later Armstrong and Strickland presented an algorithm [4] to find a suitable strobe point and calculate signal values between the sample points by the interpolation. The Maximum-likelihood estimation theory also provides a general framework for developing near-optimum synchronisation schemes [14]. A synchronisation concept shown in [10] is based on a low-order polynomial approximation of the likelihood functions using the Farrow-based interpolator. Fu and Willson in [7], instead of approximating a continuous-time signal with a conventional (algebraic) polynomial and computing the synchronised samples

integer delay

...ase of integer mismatch between output of the ...analog converters the performance of coefficients ...s affected. In the Fig. nonlinearity order $K = 7$ and the memory length between 3 [8]

...ct of integer delay for different memory length of the DPD.

...model with memory 18 a predistorter. We have ...nteger delay ranging from $\tau = -10\,Ts$ (where

We analyze the terms to integer and suitable delay between the signals used for the calculation of a DPD coefficients for predistortion. We have shown that the introduction of memory of the DPD can simultaneously compensate delay (degradation of about 3 dB compared to a NMSE of -47/dB for zero offset of τ for the Doherty amplifier studied). In the case of integer delay the synchronisation rate (the value of integer is multiple of Ts at the output of the M. But for the case of integer advance, the PMS is not able to compensate. But because the GMP is defined also for advance cross.terms, the GMP can compensate both, the integer advance and integer delay.

using a Farrow structure, employed trigonometric polynomials.

In paper [21] there are presented two methods for signal alignment in a DPD system. A frequency multiplication method was used for the coarse alignment and subsequently the parabolic curve fitting method for the fine alignment.

In this section we propose an analytical method for the fractional delay signal synchronisation and present results of its application in a DPD system. In the final section we provide experimental results of the proposed method.

4.2 Problem Observation

The described problem exists in all real systems. In coherent systems, where the clock signals in the feedback (FB) are exactly same as the clock signals in the direct path (DP), the clock phase skew can be well controlled by the design and is constant over time. The clock skew therein can be easily compensated. A different situation arises in incoherent systems where the clocks are not the same. It is to be noted that systems with clocks derived from a reference system clock by different phase-locked loops (PLLs) are considered as incoherent. A typical example of such system is an integrated transciever with separated PLLs in the transmitter and the receiver, or a measurement test-bed composed of a separated signal generator and an acquisition instrument. A simplified block diagram of such test-bed is depicted in Fig. 4.3.
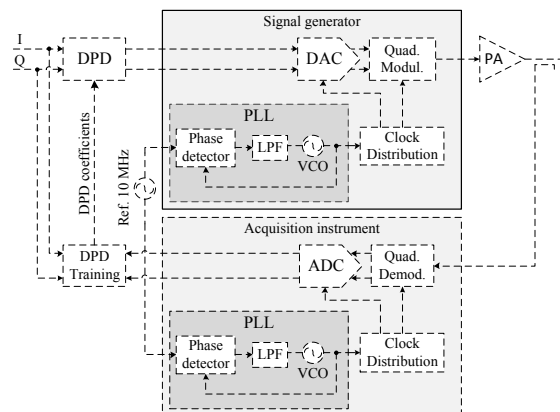
Figure 4.3: DPD test-bed with separated signal generator and acquisition instrument

The generator clock has phase skew with respect to the acquisition instrument clock. This skew is natural due to limited bandwidth of loop filters in PLLs and can vary over time. If the acquired length of the signal is relatively short with respect to the change of the clock phase skew, the phase skew can be assumed constant over the acquisition and appears as fractional sample time offset. Particularly we have observed this behaviour using high-end instruments from Rohde&Schwarz, the signal generator SMU 200A and the real-time spectrum analyser FSVR used for the acquisition. The clock phase skew spreads the amplitude-amplitude (AM/AM) characteristics as depicted in Fig. 4.4 and the amplitude-phase (AM/PM) characteristics as in Fig. 4.5. This spread can be easily misinterpreted as memory effect of the PA and it can be also partially compensated by a DPD with a memory as described in [8].
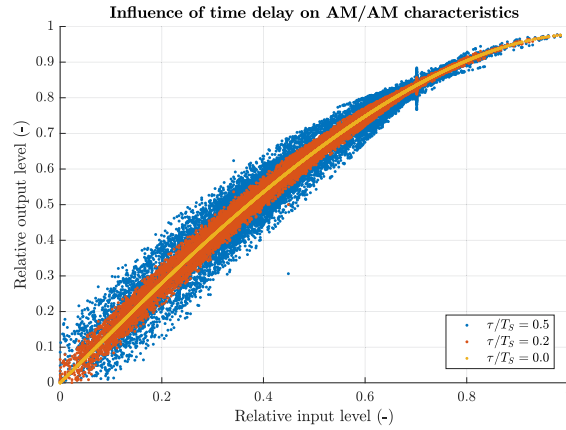
Figure 4.4: Influence of delay τ on AM/AM characteristics of PA using quadrature amplitude modulation (QAM) 16 signal with sampling period T_S
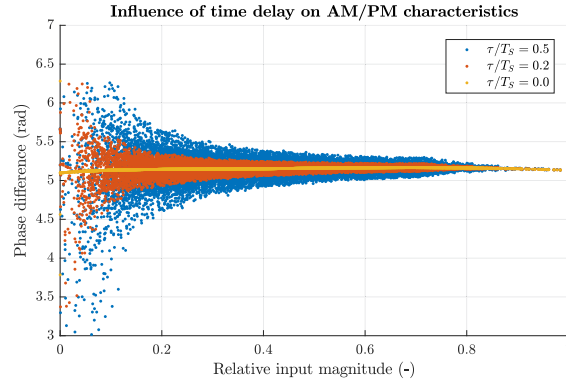
Figure 4.5: Influence of delay τ on AM/PM characteristics of PA using QAM16 signal with sampling period T_S

4.3 Proposed Synchronisation Method

Let us assume that the PA is modelled by the polynomials and its baseband output $y(t)$ is given as

$$y(t) = \sum_{k=1}^{K} \sum_{q=0}^{Q} b_{k,q} x(t - qT_S)|x(t - qT_S)|^{k-1} \tag{4.1}$$

where $x(t)$ is the PA input signal, T_S is the sampling period, K and Q represent the maximum PA nonlinear order and memory length respectively, and $b_{k,q}$ is a coefficient of the PA polynomial model. The obtained FB signal is

$$y_{FB}(t) = y(t - \tau) \tag{4.2}$$

where τ is a delay caused by the physical measurement setup and the clock skew of the instruments.

For these signals we define their Fourier transforms as

$$\mathcal{F}\{x(t)\} = X(j\omega) = |X(j\omega)|e^{j\varphi_x(\omega)} \tag{4.3}$$

and similarly $Y(j\omega)$ for $y(t)$ and $Y_{FB}(j\omega)$ for $y_{FB}(t)$. Based on Eq. 4.2 and the property of the Fourier transform it is possible to write

$$Y_{FB}(j\omega) = Y(j\omega)e^{-j\omega\tau}. \tag{4.4}$$

As the PA model (Eq. 4.1) contains only power of the magnitude, for $q = 0$ it preserves the phase of the original signal. If the memory effect of the PA is minimal and negligible, it can be shown using Eq. 4.4 that

$$\tau\omega = \varphi_x(\omega) - \varphi_{FB}(\omega). \tag{4.5}$$

For practical reasons the Eq. 4.5 is modified and the phase difference is taken from the interval $(-\pi, \pi\rangle$

$$\tau\omega = P(\varphi_x(\omega) - \varphi_{FB}(\omega)) \tag{4.6}$$

where $P(\cdot)$ is a function defined as

$$P(\varphi) = \begin{cases} \varphi \mod 2\pi, & \text{if } (\varphi \mod 2\pi) <= \pi \\ (\varphi \mod 2\pi) - 2\pi, & \text{otherwise.} \end{cases} \tag{4.7}$$

The left side of Eq. 4.6 represents a line going through the origin and with the direction τ. For real signals, τ can be found using the method of least squares and for the discrete time signals is expressed as

$$\tau_0 = \frac{\sum_{\omega_{min}}^{\omega_{max}} \omega P(\varphi_x(\omega) - \varphi_{FB}(\omega))}{\sum_{\omega_{min}}^{\omega_{max}} \omega^2} \tag{4.8}$$

where ω_{min} and ω_{max} are lower and upper limits for least squares calculation. These limits should be set according to the frequency range of the signal $x(t)$. Eq. 4.8 expects $\tau \in \langle -T_S/2, T_S/2\rangle$ which can be achieved by cross-correlation methods. The extension of the method for multiple T_S is possible by unwrapping the phase difference.

When the time offset τ_0 is obtained, the fractional sample time shift in spectrum domain is straightforward.

$$y(t) = \mathcal{F}^{-1}\{Y_{FB}(j\omega)e^{j\omega\tau_0}\} \tag{4.9}$$

The above describe approach does not change the shape of the AM/PM characteristics as Eq. 4.9 is not dependent on the magnitude of the input signal. It only improves the spread caused by the signal synchronisation offset. At the same time the method does not expect the IQ rotation of the signal phase which occurs due to the modulator and demodulator clock phase skew; therefore it is often convenient to determine τ_0 for signal magnitudes instead of complex signals.

4.4 Experimental Results

The proposed method has been experimentally verified on our measurement test-bed shown in Fig. 4.6. The test-bed consists of the signal vector generator SMU 200A, real-time spectrum analyser FSVR, both from Rohde&Schwarz, and a radio-frequency power amplifier. The reference clock for both instruments is an internal oscillator of the signal generator.
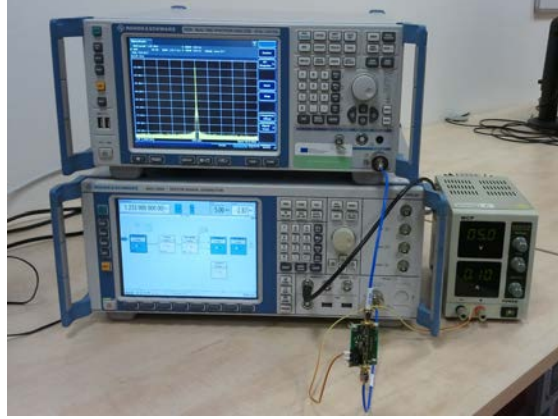
Figure 4.6: Photography of our test-bed for DPD measurements

The DPD used for the linearisation is based on the simplified 2nd-order dynamic deviation reduction (DDR) based Voltera series model [9] and its output is given by

$$
\begin{aligned}
x(n) = {} & \sum_{k=0}^{\frac{K'-1}{2}} \sum_{q=0}^{Q'} b'_{2k+1,1,q} |z(n)|^{2k} z(n-q) \\
& + \sum_{k=1}^{\frac{K'-1}{2}} \sum_{q=1}^{Q'} b'_{2k+1,2,q} |z(n)|^{2(k-1)} z^2(n) z^*(n-q) \\
& + \sum_{k=1}^{\frac{K'-1}{2}} \sum_{q=1}^{Q'} b'_{2k+1,3,q} |z(n)|^{2(k-1)} z(n) |z(n-q)|^2 \\
& + \sum_{k=1}^{\frac{K'-1}{2}} \sum_{q=1}^{Q'} b'_{2k+1,4,q} |z(n)|^{2(k-1)} z^*(n) z^2(n-q)
\end{aligned}
\tag{4.10}
$$

where $z(n)$ is an input signal to be predistored, K' and Q' are the maximum DPD non-linear order and memory length respectively, and $b'_{k,i,q}$ is a coefficient of the DPD model.

The measurements were performed first with coarse cross-correlation synchronisation only and later with application of the proposed method. The maximum nonlinear order of the DPD was set $K' = 7$ and memory length $Q' = 0$. Fig. 4.7 shows the improvement of the AM/AM characteristics for the PA before and after linearisation by usage of the proposed method. The improvement of the AM/PM characteristics of the linearised PA is shown in Fig. 4.8.
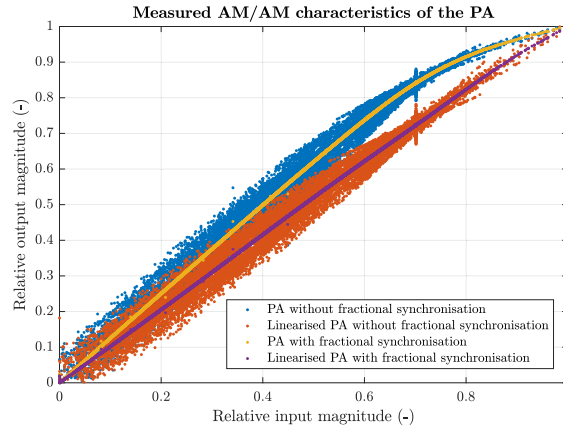
Figure 4.7: Measured AM/AM characteristics of the PA before and after linearisation with and without fractional sample period time synchronisation
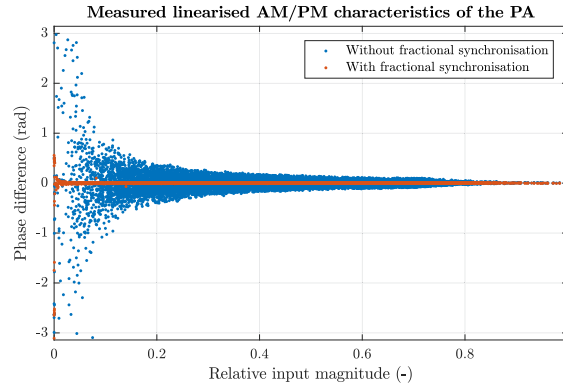
Figure 4.8: Measured AM/PM characteristics of the linearised PA with and without fractional sample period time synchronisation

Fig. 4.9 shows the phase difference (Eq. 4.6) and fitting of a line with direction τ_0. The vertical lines in this picture depict the frequency interval $\langle \omega_{min}, \omega_{max} \rangle$ which is used for the calculation of τ_0 using Eq. 4.8.

4.5 Power Amplifiers with Phase Distortion

Presence of phase distortion of the PA does not influence the performance of the proposed synchronisation method. Phase distortion in spectrum domain spreads the signals phase difference, but it preserves the direction of the fitted line. The time delay obtained using least squares is therefore insensitive to the phase distortion. Fig. 4.10 depicts a result of the synchronisation on the AM/PM characteristics of a PA with phase distortion. These characteristics were obtained by simulations only as there was no real suitable PA available for measurements.

23
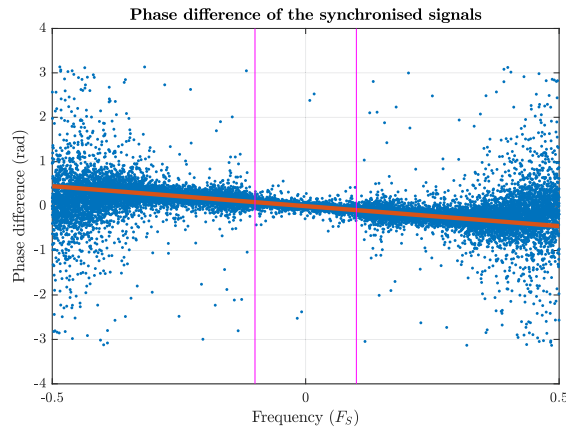
Figure 4.9: Phase difference of the synchronised signals with the fitted line representing the time offset τ_0
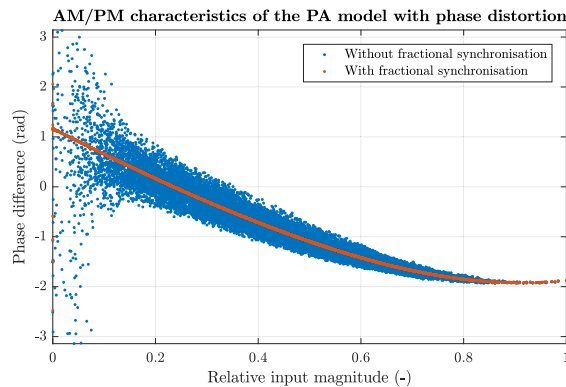
Figure 4.10: AM/PM characteristics of the PA model with phase distortion with and without fractional sample period time synchronisation. Signals without synchronisation are mutually shifted in time by $\tau/T_S = 0.48$.

4.6 Conclusion

In this section we have proposed the analytical method for fractional sample period time synchronisation using spectrum domain. It has been presented that the method, due to its properties, is suitable for time synchronisation in DPD systems suffering from incoherent sampling, e.g. integrated transcievers with separated PLLs in receiver and transmitter. The main advantage of the proposed method is that it is analytical and thus much faster than optimisation methods. We have shown application of our method in linearisation process using laboratory instruments and a real PA. The experimental measurements have shown its very good synchronisation capabilities. The simulation results have shown its outstanding performance in synchronisation of the phase distorted signals.

5. Conclusions

The DC-to-RF efficiency of High Power Amplifiers (HPAs) is currently the main contributor to the power consumption of a telecomunication systems. This equipment is responsible for consuming more than 70% of the overall DC power available in bent-pipe architectures. To improve the scenario, pre-distortion techniques are currently used in order to linearise the HPA. Such linearisation allows for an increase of the overall DC-to-RF efficiency since the HPA can be operated closer to saturation.

Feed-forward, Cartesian and Polar loop techniques provide relatively mediocre linearization performance at the expense of more complex architecture. Maturity of these techniques for wideband signals is lower compared e.g. to DPD. Moreover, as they are implemented mostly in hardware their flexibility is limited.

Digital predistortion provides very high linearisation performance. It can improve IMD3 by more than 25 dB. Since its implementation is mostly done in the digital domain and the architecture is quite straightforward, the overall system complexity and associated technical risks are mediocre. Moreover, there exists many scientific publications on the DPD and it is being deployed in several commercial applications. But in terms of reliability operating DPD for example in space would require increased number of digital components and complexity thereby reducing overall reliability.
On the other hand analogue RF predistortion that uses analogue HW components like diodes is very simple and extremely low-cost. Unfortunately it may suffer from lower linearisation performance. Improvements in IMD3 are roughly in the order of 10-25 dBc over relatively wide bandwidth. This technology is quite well matured (e.g. linearisation of TWT amplifiers in satellites). We believe that this approach should be evaluated in furtehr research works.

Usually due to low power consumption requirement, we believe that low complexity solutions such as 1-bit observing path can reduce total power dissipation significantly. This leads us to our preliminary assumption that the hybrid Analogue/Digital predistortion could be the preferred candidate for future research activities.

5.1   Research Work Beyond Thesis

The thesis includes papers which I consider the most important outputs of my research work. During my academic career, I have also been involved in other research works and authored or co-authored papers, which do not form an integral part of the presented thesis.

5.2 Bibliography

[1] Anding, Z.; Draxler, P.; Yan, J.; et al.: Open-Loop Digital Predistorter for RF Power Amplifiers Using Dynamic Deviation Reduction-Based Volterra Series. *Microwave Theory and Techniques, IEEE Transactions on*, vol. 56, no. 7, 2008: p. 1524–1534, ISSN 0018-9480, DOI:10.1109/TMTT.2008.925211.

[2] Anding, Z.; Pedro, J. C.; Brazil, T. J.: Dynamic Deviation Reduction-Based Volterra Behavioral Modeling of RF Power Amplifiers. *Microwave Theory and Techniques, IEEE Transactions on*, vol. 54, no. 12, 2006: p. 4323–4332, ISSN 0018-9480, DOI:10.1109/TMTT.2006.883243.

[3] Armstrong, J.: Symbol synchronization using baud-rate sampling and data-sequence-dependent signal processing. *IEEE Transactions on Communications*, vol. 39, no. 1, Jan 1991: p. 127–132, ISSN 0090-6778, DOI:10.1109/26.68283.

[4] Armstrong, J.; Strickland, D.: Symbol synchronization using signal samples and interpolation. *IEEE Transactions on Communications*, vol. 41, no. 2, Feb 1993: p. 318–321, ISSN 0090-6778, DOI:10.1109/26.216506.

[5] Ding, L.; Zhou, G. T.: Effects of even-order nonlinear terms on power amplifier modeling and predistortion linearization. *Vehicular Technology, IEEE Transactions on*, vol. 53, no. 1, 2004: p. 156–162, ISSN 0018-9545, DOI:10.1109/TVT.2003.822001.

[6] Ding, L.; Zhou, G. T.: Effects of even-order nonlinear terms on power amplifier modeling and predistortion linearization. *Vehicular Technology, IEEE Transactions on*, vol. 53, no. 1, 2004: p. 156–162, ISSN 0018-9545, DOI:10.1109/TVT.2003.822001.

[7] Fu, D.; Willson, A. N.: Trigonometric polynomial interpolation for timing recovery. *IEEE Transactions on Circuits and Systems I: Regular Papers*, vol. 52, no. 2, Feb 2005: p. 338–349, ISSN 1549-8328, DOI:10.1109/TCSI.2004.841573.

[8] Gotthans, T.; Baudoin, G.; Mbaye, A.: Influence of delay mismatch on digital predistortion for power amplifiers. In *Proceedings of the 20th International Conference Mixed Design of Integrated Circuits and Systems - MIXDES 2013*, June 2013, p. 490–493.

[9] Guan, L.; Zhu, A.: Simplified dynamic deviation reduction-based Volterra model for Doherty power amplifiers. In *2011 Workshop on Integrated Nonlinear Microwave and Millimetre-Wave Circuits*, April 2011, p. 1–4, DOI:10.1109/INMMIC.2011.5773325.

[10] Hamila, R.; Vesma, J.; Renfors, M.: Polynomial-based maximum-likelihood technique for synchronization in digital receivers. *IEEE Transactions on Circuits and Systems II: Analog and Digital Signal Processing*, vol. 49, no. 8, Aug 2002: p. 567–576, ISSN 1057-7130, DOI:10.1109/TCSII.2002.805630.

[11] Ibanez-Diaz, J.; Pantaleon, C.; Santamaria, I.; et al.: Nonlinearity estimation in power amplifiers based on subsampled temporal data. *Instrumentation and Measurement, IEEE Transactions on*, vol. 50, no. 4, 2001: p. 882–887, ISSN 0018-9456, DOI:10.1109/19.948293.

[12] Kim, J.; Konstantinou, K.: Digital predistortion of wideband signals based on power amplifier model with memory. *Electronics Letters*, vol. 37, no. 23, 2001: p. 1417–1418, ISSN 0013-5194, DOI:10.1049/el:20010940.

[13] Lei, G.; Zhu, A.: Simplified dynamic deviation reduction-based Volterra model for Doherty power amplifiers. In *Integrated Nonlinear Microwave and Millimetre-Wave Circuits (INMMIC), 2011 Workshop on*, 2011, p. 1–4, DOI:10.1109/INMMIC.2011. 5773325.

[14] Lin, L.; Zhang, J.; Ma, M.; et al.: Time Synchronization for Molecular Communication With Drift. *IEEE Communications Letters*, vol. PP, no. 99, 2016: p. 1–1, ISSN 1089-7798, DOI:10.1109/LCOMM.2016.2628903.

[15] Liu, Y.; Quan, X.; Pan, W.; et al.: Performance Analysis of Direct-Learning Digital Predistortion With Loop Delay Mismatch in Wideband Transmitters. *IEEE Transactions on Vehicular Technology*, vol. 65, no. 9, Sept 2016: p. 7078–7089, ISSN 0018-9545, DOI:10.1109/TVT.2015.2496188.

[16] Marsalek, R.; Jardin, P.; Baudoin, G.: From post-distortion to pre-distortion for power amplifiers linearization. *Communications Letters, IEEE*, vol. 7, no. 7, 2003: p. 308–310, ISSN 1089-7798, DOI:10.1109/LCOMM.2003.814714.

[17] Morgan, D. R.; Zhengxiang, M.; Jaehyeong, K.; et al.: A Generalized Memory Polynomial Model for Digital Predistortion of RF Power Amplifiers. *Signal Processing, IEEE Transactions on*, vol. 54, no. 10, 2006: p. 3852–3860, ISSN 1053-587X, DOI: 10.1109/TSP.2006.879264.

[18] Ngoya, E.; Quindroit, C.; Nebus, J. M.: On the Continuous-Time Model for Nonlinear-Memory Modeling of RF Power Amplifiers. *Microwave Theory and Techniques, IEEE Transactions on*, vol. 57, no. 12, 2009: p. 3278–3292, ISSN 0018-9480, DOI:10.1109/TMTT.2009.2033297.

[19] Saleh, A.: Intermodulation Analysis of FDMA Satellite Systems Employing Compensated and Uncompensated TWT's. *Communications, IEEE Transactions on*, vol. 30, no. 5, 1982: p. 1233–1242, ISSN 0090-6778, DOI:10.1109/TCOM.1982.1095568.

[20] Shimbo, O.: Effects of intermodulation, AM-PM conversion, and additive noise in multicarrier TWT systems. *Proceedings of the IEEE*, vol. 59, no. 2, 1971: p. 230–238, ISSN 0018-9219, DOI:10.1109/PROC.1971.8128.

[21] Wang, H.; Xue, W.; Ma, H.: Fast Algorithms for the Delay Estimation in Digital Predistortion System. *IEEE Microwave and Wireless Components Letters*, vol. 25, no. 3, March 2015: p. 202–204, ISSN 1531-1309, DOI:10.1109/LMWC.2015.2390532.

Abstract

The habilitation thesis is oriented in the field of modelling and linearisation of nonlinear systems. The DC-to-RF efficiency of High Power Amplifiers is currently the main contributor to the power consumption of a telecomunication systems. And since the modern communication systems are using modulation techniques with non-constant envelope (haveing high PAPR), usually back-off of power is applied in order to operate in linear region of high power amplifier. This leads to significant decrease of power efficiency. On the other hand, when operated closer to saturation the efficiency is increased, but the transmitted signal is distorted by it's non-linearity. Hence we may use linearisation techniques such as digital predistortion (imposing inverse behaviour) to improve performance.

This habilitation thesis presents research conducted at Department of Radio electronics from 2014 to 2018. First brief introduction to modelling and linearisation is provided. The second part is devoted to the analytical method for fractional sample period time synchronisation using spectrum domain. It has been presented that the method, due to its properties, is suitable for time synchronisation in digital predistortion (DPD) systems suffering from incoherent sampling, e.g. integrated transcievers with separated PLLs in receiver and transmitter. The experimental measurements have shown its very good synchronisation capabilities.

Digital predistortion provides very high linearisation performance. It can improve IMD3 by more than 25 dB. Since its implementation is mostly done in the digital domain and the architecture is quite straightforward, the overall system complexity and associated technical risks are mediocre. Moreover, there exists many scientific publications on the DPD and it is being deployed in several commercial applications.

Still there are several unanswered problems related with future systems such as 5G or 6G operating with currently large signal bandwiths. That is challenging no only in terms hardware requirements, but as well in terms of signal processing. Usually due to low power consumption requirement, we believe that low complexity solutions such as 1-bit observing path can reduce total power dissipation significantly. This fact leads us to our preliminary assumption that the hybrid analogue/digital predistortion could be the preferred candidate for future research activities.

28

Abstrakt

Habilitační práce je zaměřena na problematiku modelování a linearizaci nelineárních systémů. U telekomunikačních systémů je nízká účinnost radiofrekvenčních výkonových zesilovačů v současnosti hlavním zdrojem spotřeby energie. Dnešní moderní komunikační systémy používají modulační techniky s nekonstantní obálkou (a zároveň s vysokým PAPR). Proto, aby nedocházelo ke zkreslení signálu, je nutné snížení vysílacího výkonu (resp. snížení pracovního bodu výkonového zesilovače), proto aby bylo možno pracovat v lineární oblasti. To vede k výraznému snížení energetické účinnosti. Nicméně, když je zesilovač provozován blíže k saturační oblasti, zvyšuje se účinnost. Přenášený signál je však transformován jeho nelinearitou. Pro přenos signálů v nelineární oblasti zesilovače je možné použít linearizační techniky.

Tento dokument prezentuje výsledky výzkumu v dané oblasti prováděné na Ústavu radioelektroniky v období let 2014–2018. První část přináší stručný úvod do modelování a linearizací nelineárních systémů. Druhá část je věnována analytické metodě časové synchronizace signálů s využitím spektrální domény a demonstruje vliv na výsledky linearizace výkonového zesilovače. Díky svým vlastnostem je metoda obzvláště vhodná pro časovou synchronizaci v systémech číslicového předzkreslení (DPD) například v systémech, které trpí nekoherentním vzorkováním (integrované transceivery se samostatnými PLL v přijímači a vysílači). Experimentální měření ukázaly velmi dobré možnosti synchronizace.

Číslicové předzkreslení vykazuje velmi dobré vlastnosti z pohledu linearizování nelineárních radiofrekvenčních systémů. Může zlepšit IMD3 (intermodulační produkty třetích řádů) o více než 25 dB.

I přes relativně jednoduchou možnost implementace, existuje stále mnoho nevyřešených problémů souvisejících s budoucími systémy, jako jsou například mobilní sítě 5G nebo 6G (šířka pásma vysílaného signálu jsou řádově jednotky Ghz). To je pochopitelně náročné nejen z hlediska hardwarových požadavků, ale také z hlediska zpracování signálu. Proto je nutné se zaměřit i na nízkou spotřebu energie. Jedním z možných řešení problému mohou být systémy s nízkou složitostí, jako je 1-bitová zpětná vazba. Dalším možným řešením je použít analogové řešení. Nicméně tyto skutečnosti nás vedou k předpokladu, že preferovaným kandidátem pro budoucí výzkum v dané oblasti bude hybridní, tedy kombinace analogové a číslicové, linearizace.